Retinal Vascular Microfolds in Highly Myopic Eyes

KAORI SAYANAGI, MD, YASUSHI IKUNO, MD, FUMI GOMI, MD, AND YASUO TANO, MD

• PURPOSE: Retinal microfolds attributable to retinal vessels were first observed after vitrectomy for myopic foveoschisis and were believed to indicate inward retinal traction, possibly leading to high myopia-specific retinal diseases. We report retinal microfolds in high myopia without vitrectomy.

• DESIGN: Observational case series.

• METHODS: This is an institutional study. Seven eyes of seven patients in which retinal microfolds were observed using optical coherence tomography (OCT) were included in the study. We used an OCT-ophthalmoscope to confirm the precise location of the microfolds. We also investigated the relationship between the presence of microfolds and subjective distortion detected by examination of the corresponding retinal area using the Amsler grid chart in three eyes.

• RESULTS: All microfolds detected by OCT coincided with the retinal vessels using the OCT-ophthalmoscope. The folds coincided only with the retinal arterioles in six eyes (86%) and with both arterioles and veins in one (14%). Subjective distortion was detected in the retinal area corresponding to the microfolds in two eyes (67%) but was not detected in one eye (33%).

• CONCLUSIONS: The incidence of retinal microfolds is 2.9%, and thus they are not uncommon in highly myopic eyes without vitrectomy. The coincident appearance of the folds and vessels suggests that inflexibility of the retinal vessels and retinal stretching attributable to ocular elongation may cause the microfolds. The presence of these microfolds indicates that inward retinal vascular traction could be common in highly myopic eyes. (Am J Ophthalmol 2005;139:658-663. © 2005 by Elsevier Inc. All rights reserved.)

Accepted for publication Nov 9, 2004.

From the Department of Ophthalmology, Osaka University Medical School, Osaka, Japan.

Inquiries to Yasushi Ikuno, MD, Department of Ophthalmology E7, Osaka University Medical School, 2-2 Yamadaoka, Suita 565-0871, Osaka, Japan; fax: +81-6-6879-3458; e-mail: ikuno@ophthal.med.osaka-u.ac.jp

THE CHARACTERISTIC OCULAR STRUCTURE OF highly myopic eyes causes some peculiar vitreoretinal diseases, including myopic foveoschisis and macular hole and retinal detachment. However, it has been difficult to observe the detailed morphology of the posterior pole retina by conventional slit-lamp biomicroscopy because of chorioretinal atrophy associated with high myopia. Recent advances in instrumentation such as optical coherence tomography (OCT) and the OCT-ophthalmoscope, have revealed the nature of these diseases.[1,2]

We found retinal microfold formation after vitrectomy with internal limiting membrane (ILM) peeling for myopic foveoschisis. The microfolds were horizontal in most cases, and the location coincided exactly with the retinal arterioles, indicating the presence of inward traction exerted by the retinal vessels in high myopia, which may be related to the pathogenesis of high myopia-specific diseases such as myopic foveoschisis, paravascular microhole formation, or both.[3]

In the present study, we observed the posterior retina in eyes with high myopia but without vitrectomy using OCT and the OCT-ophthalmoscope. We found microfold formation in seven eyes, and the location of the microfolds coincided exactly with the retinal arterioles or venules. We also investigated the relation of the presence of retinal microfolds to visual disturbances detected using the Amsler grid chart.

PATIENTS AND METHODS

WE REVIEWED OCT DATA OF 239 EYES OF 130 PATIENTS WHO are followed-up at the high myopia clinic, Department of Ophthalmology, Osaka University Medical School. Retinal microfolds were found in seven eyes in the routine OCT examination and all of them are included in this study. Additional examinations such as OCT-Ophthalmoscope and/or Amsler grid charting were performed only in patients with informed consent.To obtain more detailed information about the retinal architecture and local function, OCT-Ophthalmoscope was available in all eyes (100%) and Amsler grid chart in three (43%). The

0002-9394/05/$30.00
doi:10.1016/j.ajo.2004.11.025

TABLE. Patient Demographic Data and the Presence/Absence of Retinal Microfold

Case No.	Age (y.o.)	Gender	Axial Length (mm)	Refractive Error (diopters)	BCVA	Presence/Absence of Retinal Microfolds			Amsler Grid Chart of the Corresponding Area	Visual Symptom	Other Retinal Abnormalities
						OCT (5.65 mm scan)	OCT (10 mm scan)	OCT-Ophthalmoscope			
1	70	F	NA	−17.0	20/300	+	NA	+	Normal	Visual loss	Chorioretinal atrophy
2	62	F	30.67	IOL	20/30	+	NA	+	NA	None	Chorioretinal atrophy
3	62	F	NA	−9.0	20/30	+	NA	+	Metamorphopsia	Metamorphopsia	None
4	79	M	30.27	IOL	20/30	+	NA	+	NA	Visual loss	None
5	79	F	28.21	IOL	2/200	−	+	+	NA	Visual loss	Chorioretinal atrophy
6	65	M	28.42	−16.5	20/100	+	NA	+	Metamorphopsia	Metamorphopsia	Myopic foveoschisis
7	65	F	27.87	−13.0	20/70	+	+	+	NA	Visual Loss	Chorioretinal atrophy, Choroidal neovascularization

BCVA = best-corrected visual acuity; NA = not available; IOL = intraocular lens; OCT = optical coherence tomography; + = present; − = absent.

definition of high myopia was a refractive error greater than −8.0 diopters or an axial length longer than 26 mm.

The retinal architecture was examined using OCT (Humphrey Inc., Dublin, California) and OCT-ophthalmoscope (NIDEK-OTI, Gamagori, Japan). Routine OCT examination was performed using the default setting of the crosshair mode (scan length, 5.65 mm). In two eyes (29%) (cases 5 and 7), additional OCT examination using the crosshairs mode (scan length, 10 mm) was available to obtain extended imaging of the retina.

The OCT-ophthalmoscope provides an "en face" image (C-scan) and a scanning laser ophthalmoscopy (SLO) image of the retina simultaneously, both of which represent the same part of the retina. The C-scan image can be overlaid on the SLO image using the default application of the system so that the microfolds can be located.

Three of the seven eyes (43%) were examined using the Amsler grid chart, which reflects the central retinal function 10 degrees from the fovea.[4] The presence or absence of subjective metamorphopsia, local scotoma, or both on the chart was assessed by a masked examiner.

RESULTS

PATIENT DEMOGRAPHIC DATA FROM THE SEVEN STUDY eyes are shown in the Table. There were five women and two men (mean age, 68.9 ± 7.4 years; range, 62–79 years). The mean axial length was 29.1 ± 1.3 mm (range, 27.87–30.67 mm). The axial lengths of two eyes (cases 1 and 3) were unavailable. Microfolds were detected by 5.65-mm OCT scanning in six of the seven eyes (86%) and by 10-mm OCT scanning in two eyes (29%). The OCT-ophthalmoscope detected microfolds in all eyes (100%). Visual symptoms such as visual loss (four eyes) or metamorphopsia (two eyes) were present in six eyes (86%) and absent in one eye (14%). Myopic foveoschisis was observed in one eye (14%), choroidal neovascularization was observed in one eye (14%), chorioretinal atrophy was observed in four eyes (57%), and no abnormality was observed was in two eyes (29%).

All microfolds detected by OCT scanning and the color fundus photographs from all the patients are shown in Figure 1. Microfolds could not be observed by 5.65-mm scanning in case 5 but were detected on the 10-mm OCT image. Vitreous connected to the microfolds was observed on the OCT images from two eyes (29%) (cases 1 and 4); however, the vitreous did not seem to generate tractional force on the retina in either case.

OCT-ophthalmoscopic data from all patients are shown in Figure 2. The C-scan image was overlaid on the SLO image to determine the location of the microfolds on the retina. All microfolds coincided exactly with the retinal vessels on the OCT-ophthalmoscope images. The microfolds coincided with the retinal arterioles in six eyes (86%) (cases 1, 2, 3, 4, 6, and 7), and both arteriole and venule

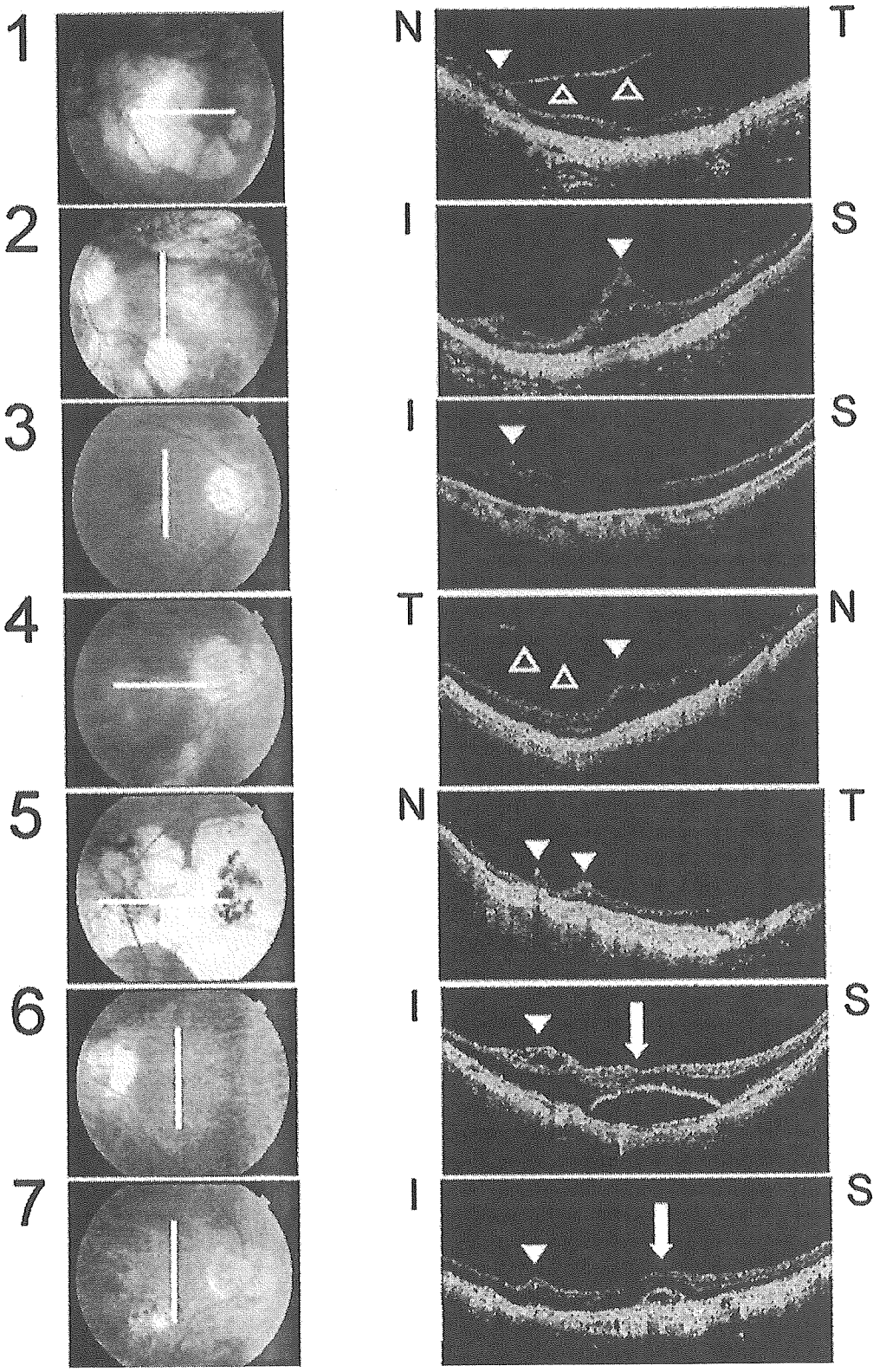

FIGURE 1. Color fundus photograph (left) and optical coherence tomographic findings (OCT, right) from each patient. (Case 1) retinal microfold (closed arrowhead) was detected by horizontal OCT scan nasal to the fovea. Posterior vitreous surface (open arrowheads) was adherent to the microfold. (Case 2) Relatively large microfold (closed arrowhead) close to the fovea was detected by vertical OCT scan. (Case 3) Microfold (closed arrowhead) was detected by vertical OCT scan presumed to be inferior to the fovea. (Case 4) Microfold was detected by horizontal OCT scan and seems to be close to the fovea (closed arrowhead). Vitreous was adherent to the microfold (open arrowheads). (Case 5) Two microfolds were detected by horizontal OCT scan (closed

in one eye (14%) (case 5), where the microfolds were at the edge of peripapillary staphyloma.

To determine if retinal microfold formation was related to visual symptoms, we examined three patients with the Amsler grid chart. The subjective distortion was present at the corresponding area involving the microfolds in two eyes (67%) (cases 3 and 6) and absent in one eye (33%) (case 1).

DISCUSSION

WE FIRST REPORTED MICROFOLD FORMATION IN EYES AFter vitrectomy and ILM peeling and presumed that the microfolds had formed as result of strong inward traction of the retinal vessels and that the traction was strengthened by increased retinal flexibility attributable to ILM peeling. Because the folds are very fine, they cannot be detected by conventional slit lamp-based examination but only by OCT or OCT-ophthalmoscope. The location of the microfolds coincided exactly with that of the retinal vessels.[3] However, in this study we observed microfolds in highly myopic eyes without vitrectomy as well, indicating that microfold formation is not specific to ILM peeling but to highly myopic eyes. We have followed 239 highly myopic eyes in our high myopia clinic, and thus far, microfolds have been found in seven eyes. The incidence of microfolds is presumed to be approximately 2.9% at present; however, additional examination including the use of extended OCT scans may enable us to find microfolds in other patients, which could increase the incidence. The incidence of microfolds is much higher in eyes after vitrectomy and ILM peeling (approximately 60%).[3] Although the reason is not yet clear, we presume that the difference could be made by ILM peeling, which is believed to make neural retina redundant.

The pathogenesis of the retinal microfolds is not known. High myopia-specific ocular structures such as posterior staphyloma formation, axial length elongation, or both are thought to be related to microfold formation. Examination using the OCT-ophthalmoscope showed that the location of the microfolds coincided exactly with the retinal vessels, which agreed with our previous report in which we found the location of the microfolds coincided with that of the retinal arterioles in all cases. However, we found that not only the retinal arterioles but also the retinal venules can generate retinal microfolds, because the microfolds coincided with the retinal venules in one (14%) of seven eyes. This suggests that not only retinal arteriolar sclerotic changes but also the inflexibility of the retinal vessels, in general, can cause this tenting traction on the retina. In two eyes, we observed the microfolds and the vitreous connected to them in OCT images. This also can be evidence that microfolds result from retinal vessels, which have relatively tight adherence to the vitreous.[5]

We hypothesized that microfold formation indicates strong inward traction because of axial length elongation in highly myopic eyes and may be related to the pathogenesis of high myopia-specific diseases such as myopic foveoschisis and paravascular microhole formation.[6] Retinal paravascular microholes in high myopia are often found at the edge of peripapillary staphyloma,[7–9] and microfold formation was found in a similar area during the OCT-ophthalmoscope examination, indicating that this traction can be a major contributor to the development of retinal holes.

The contribution of retinal vascular traction to the development of myopic foveoschisis is still unknown. We recently found that epiretinal membrane formation on the ILM may play an important role in the occurrence of foveoschisis by electron microscopic study[10] and that posterior vitreous detachment and focal vitreoretinal adhesion at the fovea causes macular holes in these eyes.[11] However, the role of vitreous traction is still questionable in developing myopic foveoschisis, although vitrectomy and ILM peeling reportedly play a role.[12,13] One case report described the spontaneous resolution of the foveoschisis attributable to posterior vitreous detachment;[14] however, this is an exceptional case in our experience. This evidence allows us to hypothesize that vascular traction can contribute to the development of myopic foveoschisis, although further investigation must be done.

We tried to evaluate how microfold formation affects visual function. Eighty-six percent of the study eyes presented with visual symptoms, and examination with the Amsler chart revealed visual abnormalities in the retina corresponding to the area involving the microfolds in 67% of the eyes with visual symptoms. However, there were co-existing abnormalities, including chorioretinal atrophy (case 1) and myopic foveoschisis (case 6), both of which can present similar findings in Amsler grid chart. This study is unable to rule out the contribution of other factors. Also, these abnormalities can cause visual symptoms in other study eyes. However

←

arrowheads). Although the location of the fovea is poorly identified due to severe chorioretinal atrophy, both seem to be nasal side of the fovea. (Case 6) Microfold was detected by vertical OCT scan (closed arrowhead). It was inferior to the fovea and seems to cause local inner retinoschisis. Myopic foveoschisis was also detected at the fovea (arrow). (Case 7) Microfold was detected by vertical OCT scan inferior to the fovea (closed arrowhead). Choroidal neovascularization, confirmed with fluorescein angiography (not shown) was also detected at the fovea.

The scan length was 5.65 mm in cases 1, 2, 3, 4, 6, and 7, and 10 mm in cases 5 and 7. The white line in the color fundus photographs indicates the optical coherence tomography scan. S = superior; I = inferior; T = temporal; N = nasal in OCT data.

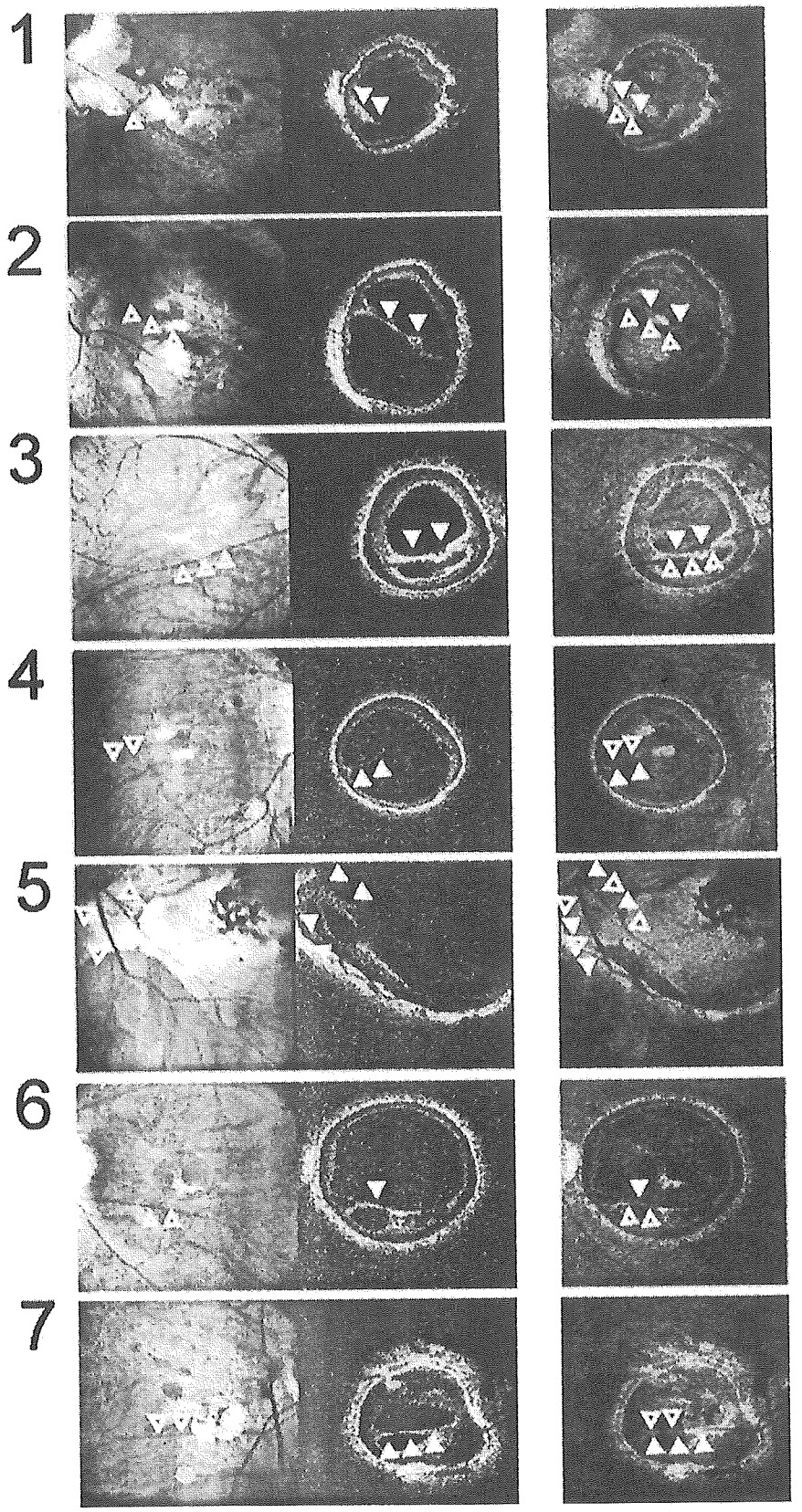

FIGURE 2. Scanning laser ophthalmoscopy (SLO) image (left) and C-scan image (middle) of the optical coherence tomography-ophthalmoscope in all patients. The C-scan image is overlaid on the SLO image using a default application (right). The open arrowheads in the left and right panels indicate retinal vessels and the solid arrowheads in the center and right panels indicate the retinal microfolds. The microfolds always coincide exactly with the retinal vessels.

there are also two cases (cases 3 and 4) in which we were aware of visual symptoms with no other abnormalities than retinal microfolds. Taken together, retinal microfolds alone are capable of causing symptoms, at least in some eyes, although additional study is needed to evaluate the impact of retinal microfolds on visual function in these eyes.

REFERENCES

1. Takano M, Kishi S. Foveal retinoschisis and retinal detachment in severely myopic eyes with posterior staphyloma. Am J Ophthalmol 1999;128:472–476.
2. Ikuno Y, Sayanagi K, Oshima T, et al. Optical coherence tomographic findings of macular holes and retinal detachment after vitrectomy in highly myopic eyes. Am J Ophthalmol 2003;136:477–481.
3. Ikuno Y, Gomi F, Tano Y. Potent retinal arteriolar traction as a possible cause of myopic foveoschisis. Am J Ophthalmol. Forthcoming.
4. Amsler M. Quantitative and qualitative vision. Trans Ophthalmol Soc U K 1949;69:397–410.
5. Spencer LM, Foos RY. Paravascular vitreoretinal attachments. Arch Ophthalmol 1970;84:557–564.
6. Favre M. Trous parapapillaires comme cause du décollement de la rétine. Ophthalmologica 1954;127:351–356.
7. Adams ST. Retinal detachment due to macular and small posterior holes. Arch Ophthalmol 1961;66:528–533.
8. Malbran E, Dodds R. Different types of holes and their significance. Bibl Ophthalmol 1967;72:170–186.
9. Regenbogen L, Stein R. Retinal detachments due to juxtapapillary microholes. Arch Ophthalmol 1968;80:155–160.
10. Bando H, Ikuno Y, Choi JS, Tano Y, Yamanaka I, Ishibashi T. Ultrastructure of internal limiting membrane in myopic foveoschisis. Am J Ophthalmol. Forthcoming.
11. Matsumura N, Ikuno Y, Tano Y. Posterior vitreous detachment and macular hole formation in myopic foveoschisis. Am J Ophthalmol. Forthcoming.
12. Kobayashi H, Kishi S. Vitreous surgery for highly myopic eyes with foveal detachment and retinoschisis. Ophthalmology 2003;110:1702–1707.
13. Ikuno Y, Sayanagi K, Ohji M, et al. Vitrectomy and internal limiting membrane peeling for myopic foveoschisis. Am J Ophthalmol 2004;137:719–724.
14. Polito A, Lanzetta P, Del Borrello M, Bandello F. Spontaneous resolution of a shallow detachment of the macula in a highly myopic eye. Am J Ophthalmol 2003;135:546–547.

Biosketch

Kaori Sayanagi, MD, graduated from Kobe University Medical School in 2001 and is now a student at the Graduate School of the Department of Ophthalmology, Osaka University Medical School. Dr. Sayanagi's research interests are in highly myopic macular disorders, including macular holes and retinal detachments, retinoschisis, and choroidal neovascularization.

REFERENCES

1. Rubenstein RA, Albert DM, Scheie HG. Ocular complications of hemophilia. Arch Ophthalmol 1966;76:231–232.
2. Kobayashi H, Honda Y. Intraocular hemorrhage in a patient with hemophilia. Metab Ophthalmol 1984–1985;8:27–30.
3. Lifshitz T, Yermiahu T, Biedner B, Yassur Y. Traumatic total hyphema in a patient with severe hemophilia. J Pediatr Ophthalmol Strabismus 1986;23:80–81.
4. Morsman CD, Holmes J. Traumatic hyphaema in a haemophiliac. Br J Ophthalmol 1990;74:563.
5. Zimmerman A, Merigan TC. Retrobulbar hemorrhage in a hemophiliac with irreversible loss of vision. AMA Arch Ophthalmol 1960;64:949–950.

Ultrastructure of Internal Limiting Membrane in Myopic Foveoschisis

Hajime Bando, MD, Yasushi Ikuno, MD, Jun-Sub Choi, PhD, Yasuo Tano, MD, Ichiro Yamanaka, MD, and Tatsuro Ishibashi, MD

PURPOSE: To reveal the pathogenesis of myopic foveoschisis (MF).

DESIGN: Clinicopathological report.

METHODS: Internal limiting membranes (ILMs) were collected from ten patients with MF and five patients with idiopathic macular hole (IMH) as a control. Samples were subjected to transmission electron microscopic study. Characteristics of the ILM were compared between the two groups.

RESULTS: Collagen fiber and cell debris were identified on the inner surface of ILM in seven eyes (70%) with MF, significantly more ($P < .05$) than found in IMH subjects (0%). More fibrous glial cells were likely to be found on the inner surface of ILM. No significant difference in fibroblast-like cell adhesion was observed.

CONCLUSIONS: Collagen fiber and cellular component are suggested to play an important role in developing MF. ILM peeling may be essential for vitrectomy for MF. (Am J Ophthalmol 2005;391:197–199. © 2005 by Elsevier Inc. All rights reserved.)

IN HIGHLY MYOPIC EYES, FOVEOSCHISIS IS TYPICALLY OBserved and thought to result in macular hole formation.[1,2] Investigators revealed that vitrectomy and internal limiting membrane (ILM) peeling is effective for foveal reattachment.[3,4] However such myopic foveoschisis (MF) is still uncertain if ILM peeling is necessary. Ultrastructural study on surgically excised specimens helps us to understand the pathogenesis. Therefore, we investigated the

Accepted for publication July 6, 2004.

From theDepartment of Ophthalmology, Graduate School of Medicine, Osaka University, Osaka, Japan (H.B., Y.I., J.S.C., Y.T.); and Department of Ophthalmology, Graduate School of Medical Sciences, Kyushu University, Fukuoka, Japan (I.Y., T.I.).

Inquiries to Hajime Bando, MD, Department of Ophthalmology E7, Osaka University Medical School, 2-2 Yamadaoka, Suita 565-0871, Japan; fax: +81-6-6879-3458; e-mail: bando@ophthal.med.osaka-u.ac.jp

TABLE 1. The Relationship between Patient Demographic Data and the Presence/Absence of Electron Microscopic Findings of Internal Limiting Membrane Excised during Vitrectomy

Case No.	Diagnosis	Age	Gender	Axial Length (mm)	Visual Acuity Data		Electromicroscopic Data (presence/absence on the inner surface of ILM)			
					Pre-op	Post-op	Cell debris*	Collagen*	Fibroblast-like cell	Fibrous glial cell
1	IMH	68	M	22.2	20/50	20/20	–	–	–	–
2	IMH	66	F	23.0	20/200	20/80	–	–	–	–
3	IMH	75	M	22.6	20/160	20/40	–	–	–	–
4	IMH	67	F	22.5	20/200	20/20	–	–	+	–
5	IMH	69	M	23.1	20/200	20/80	–	–	+	–
6	MF	70	F	31.7	2/200	20/100	+	+	+	–
7	MF	64	F	29.4	20/80	20/40	+	+	+	+
8	MF	46	F	29.2	2/100	20/125	–	–	–	–
9	MF	52	F	27.8	20/125	20/100	+	+	+	+
10	MF	46	F	28.6	20/160	20/80	+	+	–	+
11	MF	79	F	30.2	20/400	20/200	–	–	–	–
12	MF	71	F	30.6	20/800	20/100	+	+	+	–
13	MF	53	M	29.4	20/500	20/80	–	–	–	–
14	MF	63	F	27.9	20/250	20/250	+	+	–	–
15	MF	66	F	30.0	20/160	20/100	+	+	+	+

ILM = internal limiting membrane; IMH = idiopathic macular hole; MF = myopic foveoschisis; M = male; F = female; Pre-op = pre operation; Post-op = post operation; + = present; – = absent.

*Observed significantly more in MF than IMH ($P < 0.05$ by Fisher's exact test).

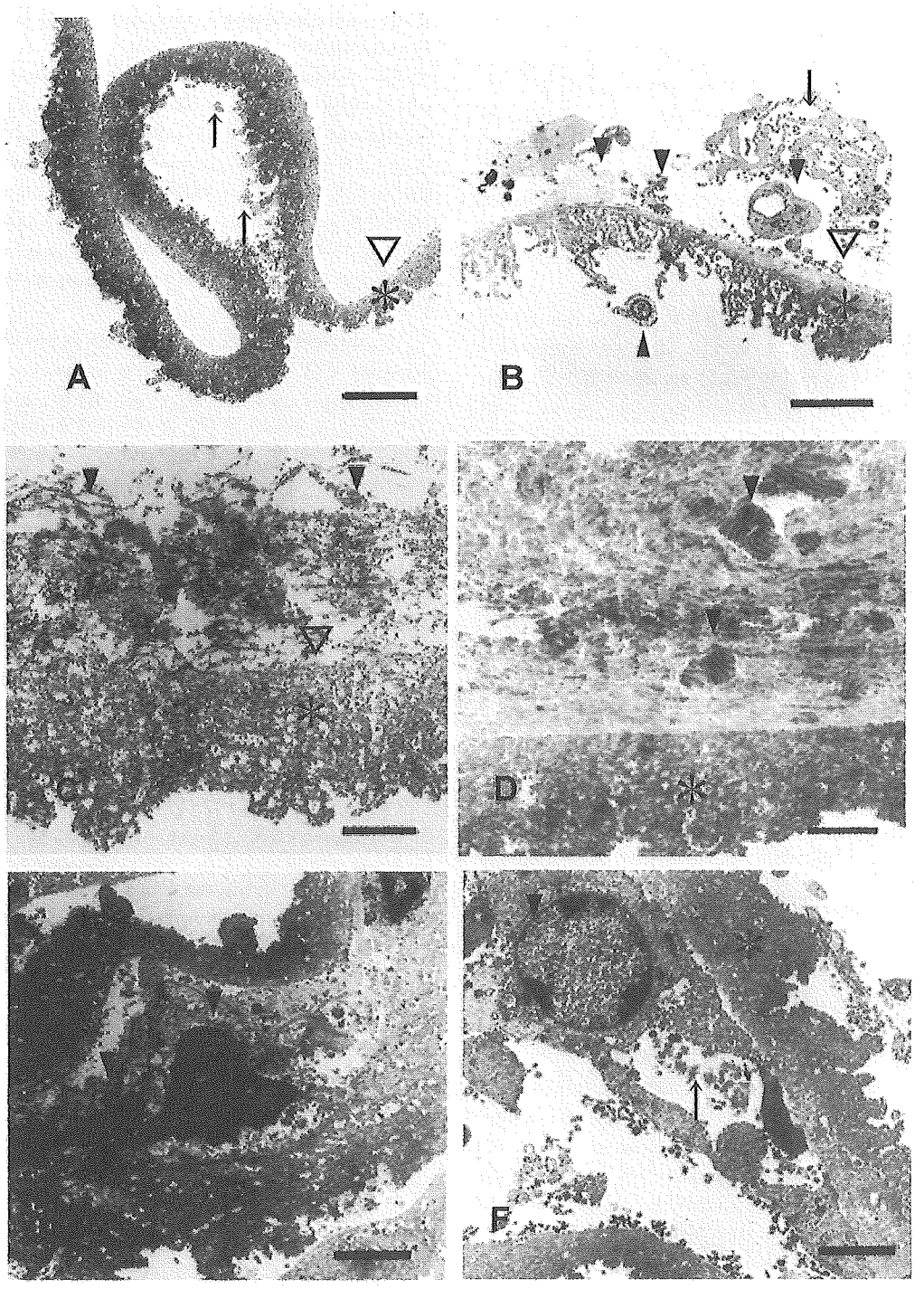

FIGURE 1. Transmission electron microscopic finding of the internal limiting membrane (ILM) excised during vitrectomy for idiopathic macular hole (IMH) or myopic foveoschisis (MF). The asterisks in A to F always indicate ILM and open arrowheads in A to C indicate the inner side of the ILM. (A) Low magnification (bar 2.8 μm, Case 3) image of the ILM from patients with IMH shows no adhering cells or collagen fibrils on the inner side. Note that the inner side of the ILM is smooth. Cell debris is observed on the outer side of ILM (arrows). (B) The photograph shows typical cell debris (closed arrowheads) and epiretinal membrane (arrow) observed on the side of ILM in an eye with MF. (bar 4.0 μm, Case 15). (C) Typical collagen fibers (closed arrowheads) adhering to the inner side of ILM from patients with MF (bar 1.2 μm, Case 12). (D) Typical long-spacing collagen from the patients with MF (arrowheads, bar 1.2 μm, Case 6). (E) Typical fibroblast-like cells (arrowheads), spindle shaped with large elongated nuclei, enmeshed in the collagen matrix, adhered to the inner side of the ILM from patients with MF (bar 2.0 μm, Case 9). (F) Typical fibrous glial cells (arrowhead) with large, regular, oval nuclei, elongated cytoplasmic processes adhered to the inner side of the ILM from patients with MF (bar 2.0 μm, Case 9). Many collagen fibrils (arrow) were present among the cytoplasmic processes.

characteristics of ILM in MF and idiopathic macular hole (IMH).

Fifteen ILMs were obtained from fifteen eyes (ten MF and five IMH) of patients who underwent vitrectomy for either MF or IMH with informed consent. All MF eyes were highly myopic, defined as a reflective error of more than −8 diopters or an axial length greater than 27 mm. Patients with diabetes mellitus, intraoperative retinal hemorrhage, were excluded. Five mg triamcinolone acetonide (TA) was injected into the vitreous cavity in all eyes with MF, but none with IMH because of difficulty in identifying the vitreous cortex in MF. Posterior vitreous detachment was created, and vitreous cortex then was removed. The ILM was stained with 0.3 ml indocyanine green (ICG, Daiichi Pharmaceutical, Tokyo, Japan) 5 mg/ml. Immediately, ICG was aspirated. ILM was peeled off using transvitreal forceps, followed by gas tamponade using expanding gas including 14% perfluoropropane (C_3F_8) or 20% sulfur hexafluoride (SF_6). We used the Accurus vitrectomy surgical system (Alcon Inc., Fort Worth, Texas) and the intensity of illumination was maintained as 80% of the default setting. Samples were fixed with 4% glutaraldehyde, and processed. We observed them under a transmission electron microscope (TEM). Statistical analysis was performed using Fisher's exact-test or Mann-Whitney U test, and $P < .05$ was considered to be significant.

Detailed patient information and the microscopic findings are shown in the Table. Cellular and extracellular components were completely absent on the inner side of ILM in three eyes (60%) with IMH (Figure 1A) and three MF eyes (30%), although cell debris was observed on the outer side in this picture (Figure 1A, arrows). Both cell debris and collagen fibers were found on the inner side in seven MF eyes (70%), significantly more than in IMH eyes (0%, $P < .05$). Cell debris was defined as a fragment of cytoplasm or cell process (Figure 1B, arrowhead). Epiretinal membrane was also found, although the morphology was not well preserved (Figure 1B, arrow). The collagen fibers are assumed to be a very fine filament (Figure 1C, arrowheads), measuring 10 to 24 nm in diameter. Moreover, one case (Case 6) had compact fibrous long-spacing collagen (Figure D, arrowheads) with a transverse banding consisting of dense lateral bars with a periodicity which in this study recorded as more than 120 nm. The major cell type found in the collagen matrix was fibroblast-like cell (Figure 1E, arrowheads). The fibrous glial cells (Figure 1F) were observed in none of the IMH eyes and in four (40%) of the MF eyes (not statistically significant, $P = .23$). There was no statistical correlation between TEM findings and visual improvement.

The current study revealed that collagen fibers were still present on the ILM in MF. Although this finding indicates the usefulness of ILM peeling to release the retina from traction, ILM peeling is suggested to be harmful for the retinal under certain circumstances.[5] For example cell debris was observed in the outer side of ILM in this study (Figure 1A).

The collagen types observed mainly on ILMs of MF were micro-fibril collagen, assumed not to be part of band formation. The micro-fibril collagen with diameters more than 20 nm seem to be newly synthesized collagen.[6] Moreover, one case exhibited compact fibrous long-spacing collagen, associated with aggregation of filamentous collagen.[7] These findings indicate that active collagen synthesis occurs on the ILM of MF probably by fibroblast-like cells and fibrous glial cells.

The reason why MF eyes presented more cellular components and collagen fibers is unknown. However, the present study indicates that cell migration and consequent collagen synthesis on the ILM can be another contributor.

REFERENCES

1. Takano M, Kishi S. Foveal retinoschisis and retinal detachment in severely myopic eyes with posterior staphyloma. Am J Ophthalmol 1999;128:472–476.
2. Ikuno Y, Tano Y. Early macular holes with retinoschisis in highly myopic eyes. Am J Ophthalmol 2003;136:741–744.
3. Kobayashi H, Kishi S. Vitreous surgery for highly myopic eyes with foveal detachment and retinoschisis. Ophthalmology 2003;110:1702–1707.
4. Ikuno Y, Sayanagi K, Ohji M, et al. Vitrectomy and internal limiting membrane peeling for myopic foveoschisis. Am J Ophthalmol 2004;137:719–724.
5. Haritoglou C, Gandorfer A, Gass CA, Schaumberger M, Ulbig MW, Kampik A. Indocyanine green-assisted peeling of the internal limiting membrane in macular hole surgery affects visual outcome: a clinicopathologic correlation. Am J Ophthalmol 2002;134:836–841.
6. Ishida S, Yamazaki K, Shinoda K, Kawashima S, Oguchi Y. Macular hole retinal detachment in highly myopic eyes: Ultrastructure of surgically removed epiretinal membrane and clinicopathologic correlation. Retina 2000;20:176–183.
7. Eyden B, Tzaphlidou M. Structural variations of collagen in normal and pathological tissues: role of electron microscopy. Micron 2001;32:287–300.

Calotropis procera (Ushaar) Keratitis

Hani S. Al-Mezaine, MD, Ali A. Al-Rajhi, MD, FRCS, FRCOphth, Abdullah Al-Assiri, MD, and Michael D. Wagoner, MD

PURPOSE: To report a case of permanent endothelial cell injury after intracorneal penetration of milky latex from *Calotropis procera* (ushaar).

DESIGN: Interventional case report.

METHODS: A 40-year-old patient developed painless corneal edema despite minimal epithelial injury after exposure to ushaar latex.

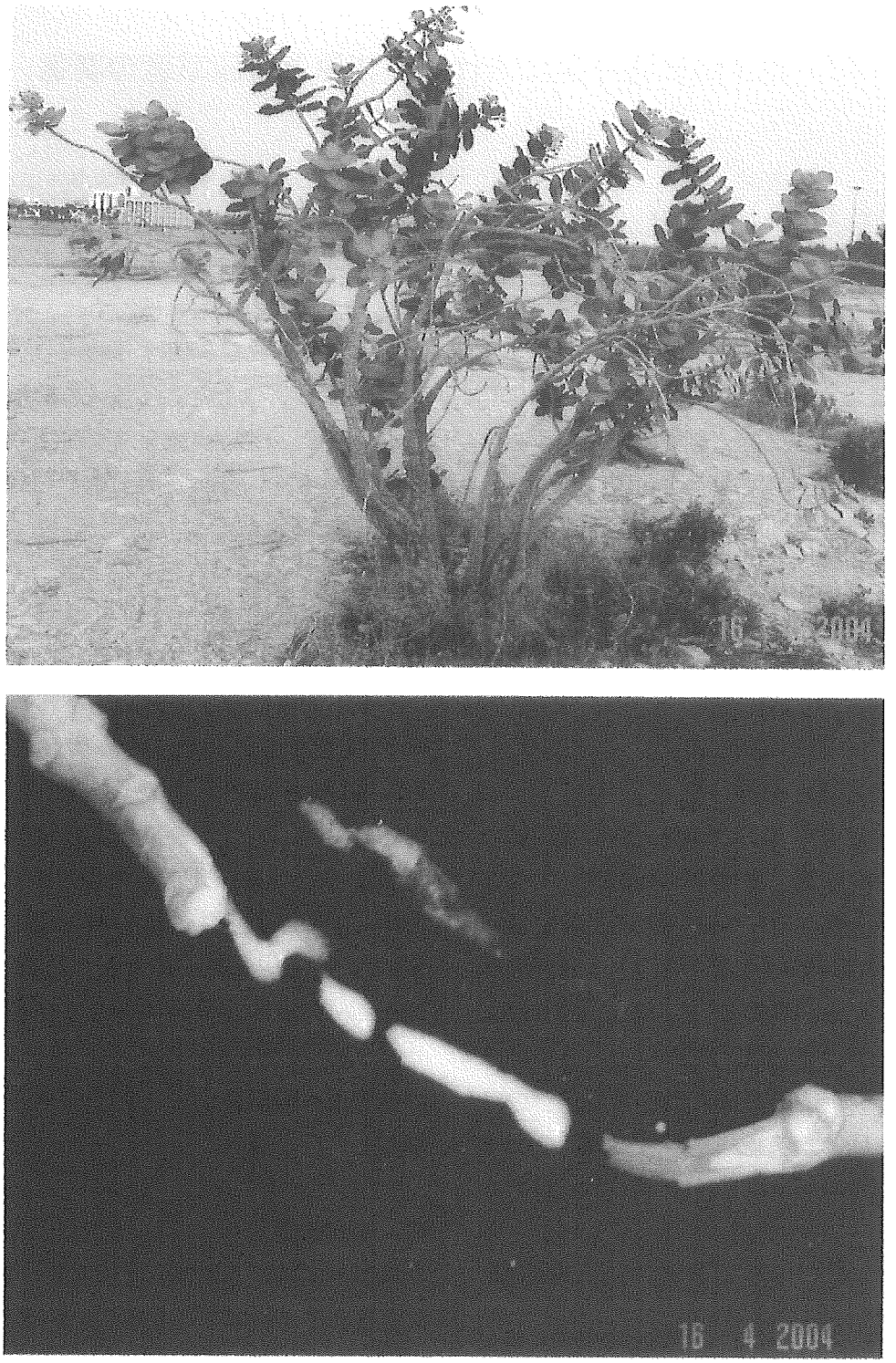

FIGURE 1. (Top) *Calotropis procera* (ushaar). (Bottom) Milky latex from cut branch.

12. 糖尿病黄斑浮腫における網膜厚と網膜感度の関係

野本浩之、蔭山光代、白神千恵子、山下彩奈、山地英孝、白神史雄
(香川大)

研究要旨　糖尿病黄斑浮腫における網膜厚と網膜感度の関係を検討するために、中心窩から直径 6mm 以内の領域の網膜厚を光干渉断層計を用いて測定し、対応する領域の平均網膜感度を新しい微小視野計である Microperimetry 1 を用いて計測した。各領域の網膜厚と網膜感度は負の相関関係を認めたが、ばらつきは大きかった。黄斑浮腫を形態別に分類した場合、cystoid macular edema 型でもっともばらつきが小さく、serous retinal detachment 型では有意な相関関係を認めない結果となった。

A. 研究目的

糖尿病黄斑浮腫における網膜厚と網膜感度の関係を検討すること。

B. 研究方法

対象は発症後 1 年以内の糖尿病黄斑浮腫の患者 26 例 33 眼。男性 16 例 20 眼、女性 10 例 13 眼、年齢 51-76 歳(平均 58.8 ± 11.8 歳)、眼力は 0.04-1.2、平均中心窩網膜厚は 239-927μm(平均 517 ± 142μm)であった。光干断層計検査(OCT, ZEISS 社)から黄斑浮腫を分類すると、びまん性浮腫型(diffuse 型)は 16 眼、嚢胞様黄斑浮腫型(CME 型)は 9 眼、浸出性網膜剥離型(SRD 型)は 8 眼であった。

網膜厚は光干渉断層計の Fast Macular Thickness Map で 6mm×6 スキャンし Retinal Map プログラムで中心窩から直径 6mm を 9 領域に分け (図 1)、それぞれの平均網膜厚を測定した。網膜感度は Micro Perimetry 1 (MP1; ニデック社) を用いて OCT の 6 スキャンの角度にあわせた測定点 (図 2) を、Retinal Map の各領域で最低 6 点は測定するように合計で 37 点設定した。刺激は Goldmann III の大きさで 200msec、Threshold Strategy は 4-2-1 で行った。

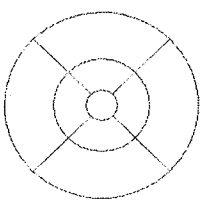

図 1:OCT の 9 領域

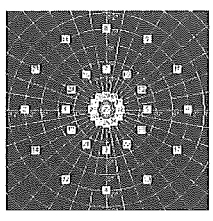

図 2:MP1 の測定点

(倫理面への配慮)

なし

C. 研究結果

各領域の網膜厚と網膜感度の有意な負の相関を認めたが、ばらつきは大きかった (r2=0.298; p<0.0001) (図 3)。

また、中心窩から直径 1mm 以内の領域、2-3mm の領域、3-6mm の領域別の相関関係、ばらつきは同程度であった (r2=0.246-0.320)。

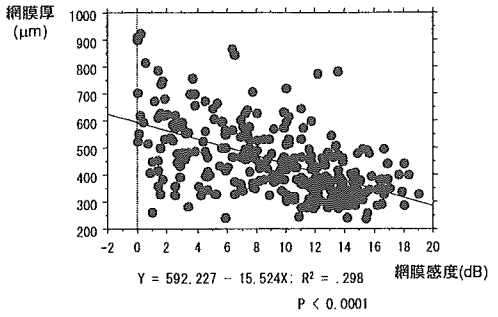

図 3: 網膜厚と網膜感度の相関

黄斑浮腫の形態別では、diffuse 型では同程度であったが(図 4: r^2=0.299; p<0.0001)、CME 型ではばらつきが少なく (図 5: r^2=0.492; p<0.0001)、一方 SRD 型では有意な相関関係は認められなかった(図 6: r^2=0.011; p=0.37)。

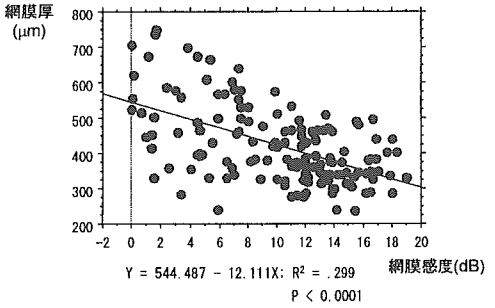

図 4: diffuse 型の網膜厚と網膜感度の相関

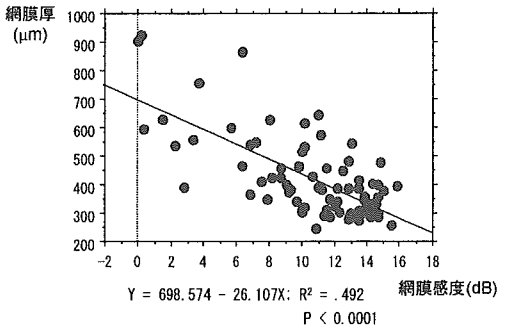

図 5: CME 型の網膜厚と網膜感度の相関

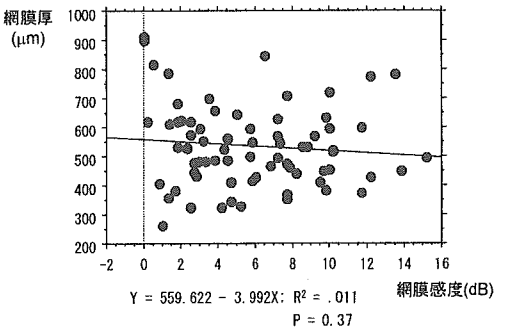

図 6: SRD 型の網膜厚と網膜感度の相関

【結論】糖尿病黄斑浮腫において、各領域の網膜厚とそれに対応する網膜感度は有意な相関関係があるものの、ばらつきは大きかった。黄斑浮腫の形態別では CME 型ではばらつきが少なく、SRD 型では有意な相関関係を認めなかった。

D. 考察

MP-1 は新しく開発された微小視野計で、その特徴は検査時時間が短く、自動トラッキングシステムによって眼球が動いても同じ部位を刺激できることや、眼底写真と検査結果を重ね合わせることによって眼底に対応した部位での網膜感度を表示できることである。[1-3] また、現在、黄斑浮腫の定量は OCT3000 の Retinal Map プログラムで中心窩から直径 6mm 以内の範囲を 9 領域に分けて解析することが多い。そこで我々は MP1 のエディット機能を用いて OCT の Fast Macular Thickness Map のスキャンラインにあわせた測定点を設定することで、Retinal Map に対応した領域の平均網膜感度を算出した。

網膜厚と網膜感度は有意でかつ負の相関関係を示したが、寄与率 (R^2)は小さくばらつ

きが大きかった。網膜感度には網膜厚が関与しているのことが考えられたが、それ以外の要因も影響している可能性が示唆された。

黄斑浮腫を OCT で形態別に分類した場合、CME 型では寄与率が大きい結果となった。これは、CME 型では浮腫が黄斑部に限局しており、正常部位を多く含んでいることが一因になっていることが考えられる。また、SRD 型は唯一有意な相関関係を認めなかった。これは、網膜厚を網膜色素上皮から網膜内境界膜までの厚みを網膜厚として計算していることから、網膜下液を網膜厚に含めていることが要因となっているのかもしれない。

E. 結論

糖尿病黄斑浮腫において、各領域の網膜厚とそれに対応する網膜感度には負の相関関係を認めたものの、高い相関関係は示さなかった。

F. 健康危険情報

なし

G. 研究発表

1. 論文発表

なし

2. 学会発表

野本浩之他：糖尿病黄斑浮腫における網膜厚と網膜感度の関係　第 44 回日本網膜硝子体学会, 大阪市, 2005

H. 知的財産権の出願・登録状況

1. 特許取得

なし

2. 実用新案登録

なし

3. その他

なし

I. 参考文献

1. Rohrschneider K et al: Microperimetry-comparison between the micro perimeter 1 and scanning laser ophthalmoscope-fundus perimetry. Am J Ophthalmol 139: 125-134, 2005.
2. Springer C et al: Fundus perimetry with the Micro Perimeter 1 in normal individuals: comparison with conventional threshold perimetry. Ophthalmology 112: 848-854, 2005.
3. Okada K et al: Correlation of retinal sensitivity measured with fundus-related microperimetry to visual acuity and retinal thickness in eyes with diabetic macular edema. Eye 15: 1-5, 2005.

13. 抗高脂血症薬による黄斑浮腫治療の試み

村田敏規、千田奈実、片井直達、千葉　大、京本敏行、山本裕香
(信州大)

研究要旨　近年硝子体手術の進歩により、糖尿病網膜症の直接的な失明原因である、牽引性網膜剥離と血管新生緑内障は、多くの症例で手術的に対処できる疾患になりつつある。しかし、こういった症例の多くは黄斑浮腫を伴っており、読書や運転などが可能な良好な視力は維持できない。現在黄斑浮腫の治療法としては、黄斑部の網膜光凝固や硝子体手術が行われているが、硬性白斑が中心窩に沈着するとこれが視細胞を破壊し中心視力は著しく低下する。網膜光凝固や硝子体手術の補助療法として、高脂血症を改善させることが硬性白斑の沈着や黄斑浮腫の改善につながると考え研究を行っている。

A．研究目的

網膜光凝固で糖尿病網膜症を治療するにあたり、高脂血症を治療することが黄斑浮腫に与える影響を検討する。

1) 高脂血症を治療することで、黄斑浮腫は軽減するか否かを検討する

2) 経過観察中、無灌流領域の形成に伴う網膜血管新生の出現や、網膜細動脈瘤の増加により、黄斑浮腫が悪化した場合は必要に応じて網膜光凝固を行う。この場合は網膜光凝固と高脂血症の治療の併用効果を検討することになる。最終的に中心窩に硬性白斑が沈着しなければ治療は成功とする。

B．研究方法

以下の条件に適合する患者を対象とする。

1）硬性白斑を伴う糖尿病黄斑浮腫。

2）高脂血症を伴う糖尿病。

3）抗高脂血症薬を内服していない。

4）過去３ヶ月以内に網膜光凝固や眼内手術歴がない。

Informed consent をとりHMG-CoA還元酵素阻害薬 pitavastatin を投与開始し、３ヶ月に一度、眼科的には硬性白斑と黄斑浮腫を評価する目的で下記のような検査行った。眼底写真、optical coherence tomography の retinal thickness map で黄斑浮腫による網膜の肥厚を評価。蛍光眼底造影による黄斑浮腫の評価、視力検査でもうまく機能の評価。内科的には血清脂質、血糖値、HbA1c を評価し、肝機能などの副作用のチェックをおこなう。

(倫理面への配慮)

高脂血症はほとんどの糖尿病患者が合併して持っている病気である。高脂血症の改善が動脈硬化の予防につながり、心筋梗塞や脳梗塞の予防につながることをほとんどの患者様が知識としては持っておられるが、高脂血症を治療は受けていない患者が多い。高脂血症を治療することはご本人の利益になることを説明し、内科医と連携して高脂血症の治療に当たる。

C．研究結果

HMG-CoA 還元酵素阻害薬 pitavastatin の投与を開始すると、全例で短期間で高脂血症の改善がえられた。

現在 4 例 6 眼がエントリーして、6 ヶ月以上経過を追うことができているのは、2 例 3 眼である。以下 retinal thickness map で網膜浮腫の変化を示す。

図 1　中心窩周囲で、浮腫を示す黒い部分が減少

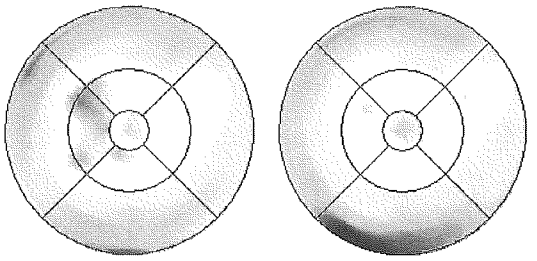

この眼は高脂血症の治療のみで黄斑浮腫が軽減し、6 ヶ月これを維持している。

図 2 中心窩付近の強い浮腫を示す白い部分が減少

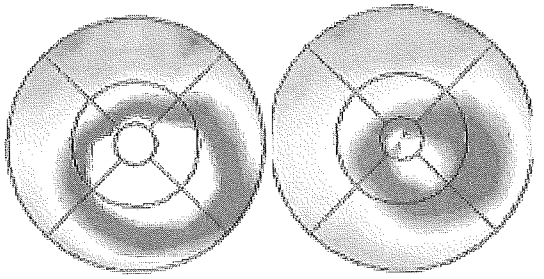

この眼図 2 の右側のように、3 ヶ月までは高脂血症の改善に伴い、中心窩付近で、白色に描出されている網膜の強い浮腫が軽減している。しかし、無灌流領域の形成があり、観察期間が 6 ヶ月を超えているので、網膜光凝固を施行する予定である。

図 3　6 ヶ月で光凝固を併用した例

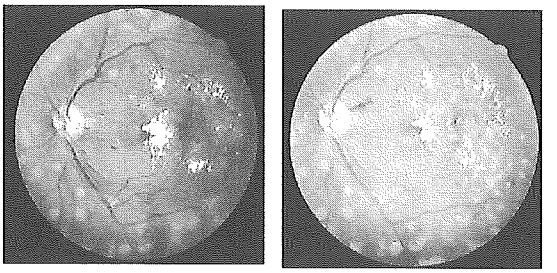

この症例は中心窩を取り囲むように硬性白斑が存在し、高脂血症改善で中心窩を取り囲む硬性白斑は減少する傾向がみられた。しかし、無灌流領域の形成と血管新生がみられて網膜光凝固を施行している。

D．考察

HMG-CoA 還元酵素阻害剤を投与して、高脂血症を治療すると、黄斑浮腫の改善や硬性白斑の減少を示す傾向が見られた。しかし、3 眼中 2 眼で無灌流領域形成にともなう網膜浮腫の悪化が出現し、網膜光凝固の施行が必要であった。

網膜光凝固を併用した 1 眼では、中心窩を硬性白斑が 180° 以上とり囲んでいたが、高脂血症の治療と網膜光凝固の併用で、中心窩に硬性白斑を沈着させることなく治療できた。

今後症例数を増やして検討する必要があるが、高脂血症の改善は網膜光凝固と併用することで、黄斑浮腫の改善および硬性白斑が中心窩に沈着するのを防ぐ効果がある可能性が示唆された。

E．結論

糖尿病黄斑浮腫の患者の高脂血症を HMG-CoA で改善させることは、網膜光凝固の補助療法として有効である可能性がある。

F．健康危険情報

なし

G．研究発表

1．論文発表

なし

2．学会発表

1. 抗高脂血症薬による黄斑浮腫の治療
   千田奈実他　第 5 回 Tokyo Retina Club 東京　2005

H．知的財産権の出願・登録状況

1．特許取得

なし

2．実用新案登録

なし

3．その他

なし

I．参考文献

なし

14. Retinal Angiomatous Proliferation (RAP) に対する網膜血管切断術後の網膜循環の変化

森 隆三郎、川村昭之、島田宏之、中田光紀、湯沢美都子
(日本大)

研究要旨 目的：Retinal Angiomatous Proliferation (RAP) に対して新生血管と吻合する網膜流入血管と流出血管を切断する外科的治療後の新生血管付近の網膜循環の変化を明らかにする。対象と方法：RAP と診断し、硝子体手術時に網膜流入血管、流出血管を切断した 3 例 3 眼について、術前と術後のフルオレセイン蛍光造影検査およびインドシアニングリーン蛍光造影検査の所見を比較検討した。結果：流入血管、流出血管を切断できた 2 眼の血流は減少し、新生血管は縮小したが、切断部の末梢側の流入血管と流出血管が造影されていた。血流方向は、周囲の網膜動脈から切断された流出血管、新生血管、流入血管の順で、術前と逆になっていた。流入血管のみを切断した 1 眼でも、血流は減少し、新生血管は縮小した。網膜動脈より網膜毛細血管、切断された流入血管、新生血管の順で造影されていた。結論：RAP の網膜流入血管と流出血管を切断すると、新生血管は縮小するが、新生血管への血流は途絶しなかった。

A. 研究目的

Retinal Angiomatous Proliferation (RAP) に対して Borrillo は新生血管への網膜流入血管と流出血管を切断する治療法を報告した[1]。しかし、黄斑部には発達した中心窩周囲毛細血管網があり、流入血管と流出血管を切断しても新生血管への血流が途絶するかは、疑問である。そこで、RAP に対して新生血管と吻合する網膜流入血管と流出血管を切断する外科的治療後の新生血管付近の網膜循環について検討した。

B. 研究方法

対象は、Heidelberg 社製走査レーザー検眼鏡 (HRA) の High-Speed Indocyanine green angiography (IA) と Fluorescein angiography (FA) で、RAP と診断した 3 例 3 眼。術前に IA で同定できた流入血管、流出血管を切断し、その断端をジアテルミーで凝固した。HRA で術前と術後 1 か月に FA 、IA を行い、新生血管付近の網膜循環の変化を調べた。

(倫理面への配慮)

患者に本治療が RAP に対する新しい治療方法の一つであることを含め手術に関して書面によるインフォームドコンセントを得た。

C. 研究結果

Ⅰ. 流入血管、流出血管を切断した 2 眼は、血流は減少し、新生血管は小さくなってい

た。しかし、切断部より末梢側の流入血管、流出血管が造影されていた。造影は、周囲の網膜動脈、切断された流出血管、新生血管、切断された流入血管の順であり、血流方向は、術前と逆になっていた。

症例１：81 歳女性、左眼矯正視力 0.1、RAP stage３。IA では、新生血管は hot spot と呼ばれる過蛍光斑を示し、新生血管と網膜血管の吻合も明瞭で、流入血管（矢印A）と流出血管（矢印B）が造影されている。矢頭の部位で流入血管と流出血管を切断した。術前後のＩＡ早期像を比較すると、術前は、耳側の動脈に造影剤が流入し、鼻側の静脈から流出しているが、術後は、切断された流出血管に造影剤が入り（矢印C）、耳側の流入血管から流出している（矢印D）。すなわち、血流方向は、術前と逆になっている。新生血管は縮小している。（図１）

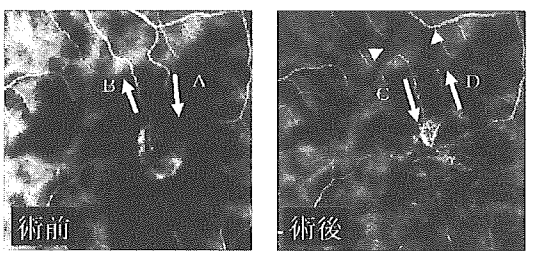

図１　症例１　術前後のＩＡ早期像

症例２：88 歳男性。右眼矯正視力 0.1 、RAPstage2。IA では、１本の流入血管（矢印A）と２本の流出血管（矢印B、C）が造影されている。矢頭の部位で流入血管と流出血管を切断した。その末梢側の流出血管（矢印D）、流入血管（矢印E）は造影され、血流方向は、術前と逆になっている。新生血管は縮小している。（図２）

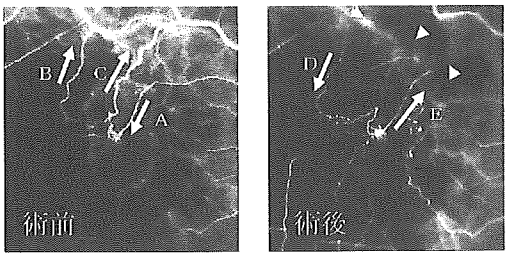

図２　症例２　術前後のＩＡ早期像

Ⅱ．結果的に流入血管のみを切断した１眼は、血流は減少し、新生血管は小さくなっていた。切断部より末梢側の流入血管が造影されており、周囲の網膜動脈から、毛細血管、切断された流入血管を介して新生血管に血流が流入していた。

症例３：８５歳女性。左眼矯正視力 0.０４、RAP stage2。FA では、新生血管と網膜血管の吻合も明瞭で、流入血管（矢印A）と流出血管（矢印B）が造影されている。流入血管（矢頭の部位）と流出血管の切断を試みたが、流出血管は切断されていない。術後、上方の網膜動脈より毛細血管、切断された流入血管（矢印 C）を介して新生血管に造影剤が流入している。血流方向は、術前と逆になっていない。新生血管は縮小し、黄斑浮腫は改善している。（図３）

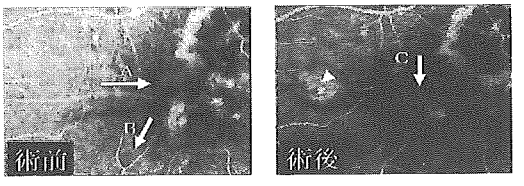

図３　症例３　術前後のＦＡ早期像

Ｄ．考察

RAP は、２００１年に Yannuzzi らが、網膜血管由来の新生血管を有する加齢黄斑変性

の特殊型として報告している[2)]。治療は、新生血管が、中心窩にある場合はトリアムシノロン硝子体内あるいはテノン嚢下注入、光線力学的療法、光線力学的療法とトリアムシノロン注入併用療法が行われている。一方、新生血管への網膜流入血管と流出血管を切断する方法は、Borrillo らが stage 2 の４症例に対して有効であったと報告した[1)]。Boscia らは、stage 3 の１例について[3)]、Sakimoto らは、stage2 に対する 術後 6 か月で新たな網膜血管と新生血管の吻合を認めた 1 例について報告している[4)]。しかし、新生血管付近の網膜循環の変化についての報告はない。今回、我々は、新生血管への流入血管と流出血管を切断した場合に、術後 1 か月の時点で、黄斑部の発達した中心窩周囲毛細血管網の領域で、新生血管への血流が途絶しているかを調べた。３症例全てで新生血管が縮小し、黄斑浮腫が改善したのは、流入血管を切断したことにより、網膜主幹動脈から新生血管へ直接流入する血流が減少したためであると推察した。流入血管、流出血管を切断した２眼では、切断部より末梢側の流入血管と流出血管が造影され、造影は、周囲の網膜動脈、切断された流出血管、新生血管、切断された流入血管の順で、血流方向は、術前と逆になっていた。その理由として、静脈圧は動脈圧よりも低くまた切断後は血流が途絶しているため抵抗が少なく、動脈血が周囲の毛細血管網を介して切断した静脈に流入し易いと推察した。また結果的に流入血管のみを切断した１眼では、造影は、周囲の網膜動脈から毛細血管を介して切断部より末梢側の流入動脈、新生血管の順であった。その理由として、切断後は流入血管の血流が途絶しているため抵抗が少なく、周囲の毛細血管網の動脈血が切断部より末梢側の流入血管に流入し易いと推察した。

E. 結論

RAP に対して新生血管と吻合する網膜流入血管と流出血管を切断すると、網膜血管からの血流は減少し、新生血管は縮小するが、網膜血管からの血流は途絶しないことが明らかになった。

F. 健康危険情報

なし

G. 研究発表

1. 論文発表

なし

2. 学会発表

1. 川村昭之 他：Retinal Angiomatous Proliferation（RAP）に対する硝子体手術術後の網膜循環の変化、第 58 回日本臨床眼科学会、東京、2004
2. Mori R, et al : The retinal circulation after surgical disconnection of retinal angiomatous proliferation, 8TH Michaelson Symposium, Gent. Belgium, 2005

H. 知的財産権の出願・登録状況

1. 特許取得

なし

2. 実用新案登録

なし

3. その他

なし